

# 넓은 입력 전압 범위와 감소된 스트레스 전압 가능성을 갖는 새로운 승압형 멀티레벨 DC-DC 컨버터

이바둘라예브 안바르<sup>1</sup>, 박성준<sup>†</sup>

## A New Multi Level High Gain Boost DC-DC Converter with Wide Input Voltage Range and Reduced Stress Voltage Capability

Ibadullaev Anvar<sup>1</sup> and Sung-Jun Park<sup>†</sup>

### Abstract

The use of high-gain-voltage step-up converters for distributed power generation systems is being popularized because of the need for new energy generation and power conversion technologies. In this study, a new constructed high-gain-boost DC - DC converter was proposed to coordinate low voltage output DC sources, such as PV or fuel cell systems, with high DC bus (380 V) lines. Compared with traditional boost DC - DC converters, the proposed converter can create higher gain and has wider input voltage range and lower voltage stress for power semiconductors and passive elements. Moreover, the proposed topology produces multilevel DC voltage output, which is the main advantage of the proposed topology. Steady-state analysis in continuous conduction mode of the proposed converter is discussed in detail. The practicability of the proposed DC - DC converter is presented by experimental results with a 300 W prototype converter.

**Key words:** High gain boost DC-DC converter, High efficiency, Multilevel DC-DC converter, Switched capacitor, Reduced stress voltage

### 1. Introduction

Recently, with the development of green energy producing technology, the use of renewable sources such that PV arrays, fuel cells, etc. have been increasing rapidly. Since the output voltage level of the renewable sources is very low, two stage power conversion is required to generate high DC bus (380V) shown in Fig. 1. In the first stage low level DC voltage is increased to a high level DC voltage (380V) by power converter with a high gain conversion and high efficiency. In the second stage high DC voltage can be used for DC or AC voltage application.

The traditional boost converters have not high gain capability to make high DC voltage as they require high duty cycle, which resulted in high power loss and reduced life cycle. To get a high gain and high efficient power converter, there are developed many converters, such that isolated, non-isolated and also floated output step-up converters<sup>[1]-[4]</sup>. The isolated circuits have some disadvantages, that they require a large number of components to make high DC voltage in two stage. And also the isolated boost converters demand briefly parameters design which will be difficult. Non-isolated converters step up low voltage in many techniques, such that switched-inductor (SL) based, switched-capacitor (SC) and mixed types<sup>[5]-[7]</sup>. The topologies certainly have high gain capability, but on the other hand have some disadvantages, such that large number of components, high voltage stress, high input current ripple and complexity of the circuit. Such disadvantages lead to high cost and decreases device life cycle.

Paper number: TKPE-2020-25-2-9

Print ISSN: 1229-2214 Online ISSN: 2288-6281

<sup>†</sup> Corresponding author: sjpark1@chonnam.ac.kr, Dept. of Electrical Engineering, Chonnam Nat'l University  
Tel: +82-62-530-1741 Fax: +82-62-530-1189

<sup>1</sup> Dept. of Electrical Engineering, Chonnam Nat'l University.  
Manuscript received Dec. 30, 2019; revised Jan. 7, 2020;  
accepted Feb. 19, 2020

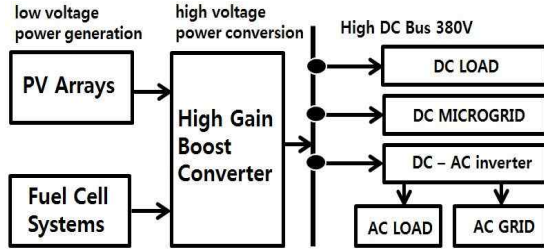


Fig. 1. Block diagram of a typical power generation system.

In order to obtain high gain, high efficient and low voltage stress topologies, Voltage Multiplier, Voltage lift, Multilevel output and X-shaped Z-source network converters were developed<sup>[8]-[12]</sup>. Such converters has high gain, high flexibility and  $\frac{1}{2} V_{out}$  stress voltage. However, some components suffer from  $V_{out}$  equal voltage and high current stress. And also the duty value of such converters approaches to unity which will lead to high power losses. Because of such disadvantages there is a need to create some boost converter which can obtain high gain capability with lowered number of active and passive elements and decreased duty cycle.

The goal of this paper is to create high gain, high efficient, long life cycle and wide input voltage range boost dc-dc converter by

- ① decreasing all components voltage stress from  $V_{out}$  to  $\frac{1}{3} V_{out}$  value;
- ② decreasing duty  $D$  cycle;
- ③ creating multilevel output DC voltage.

This paper will be described in the following sequence. Section 2 presents the proposed converter topology, operating principles and some analysis. Simulation results are in Section 3. Comparisons to other boost converters is discussed in Section 4. Active and passive components selection will be described in Section 5. In Section 6 experimental results will be described. Finally, in Section 7 a few conclusions will be described.

## 2. The Proposed Converter Topology and Some Operating Analysis

### 2.1 Circuit of the proposed converter

The proposed converter topology is made by two MOSFETs  $S_1$  and  $S_2$ , inductor  $L$ , capacitors  $C_{UP}$ ,  $C_{o1}$ ,  $C_{o2}$ ,  $C_1$ ,  $C_2$ , diodes  $D_1$ ,  $D_2$ ,  $D_3$  and  $D_{out}$  as pictured in Fig. 2. The output capacitors  $C_{o1}$  and  $C_{o2}$  are connected

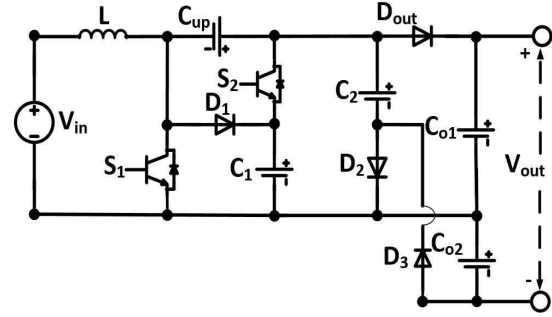


Fig. 2. Proposed high gain multi level boost converter.

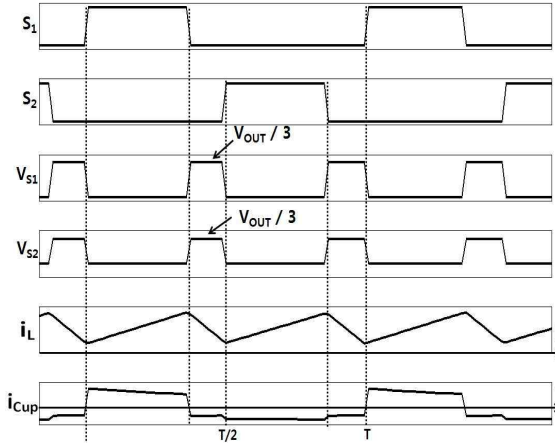


Fig. 3. Main waveforms of the proposed converter for CCM operation.

in series.  $C_{o1}$  capacitor have common ground with the input DC source, but  $C_{o2}$  capacitor has different ground. This connection let to create multilevel output capability and thus decreases voltage stress for active and passive components. Capacitor  $C_{UP}$  is connected in switched-capacitor technique. The main waveforms of the proposed topology are presented in Fig. 3. As shown in the Fig. 3.  $S_1$  and  $S_2$  switches drain-source voltages  $V_{S1}$  and  $V_{S2}$  are equal to third value of output DC voltage, the inductor current is twice charged and discharged during one switching period. And there is no inrush current in  $C_{UP}$  capacitor.

In order to explain the steady state operation of the proposed converter, some assumptions are made as below :

- ① The effects of ON state resistance ( $R_{DS(ON)}$ ) of the switches, forward voltage drop ( $V_f$ ) of the diodes and equivalent series resistance ( $ESR$ ) of the inductor and electrolytic capacitors are neglected ;
- ② The summarized capacitance of the two output capacitor are enough to maintain constant output DC voltage.

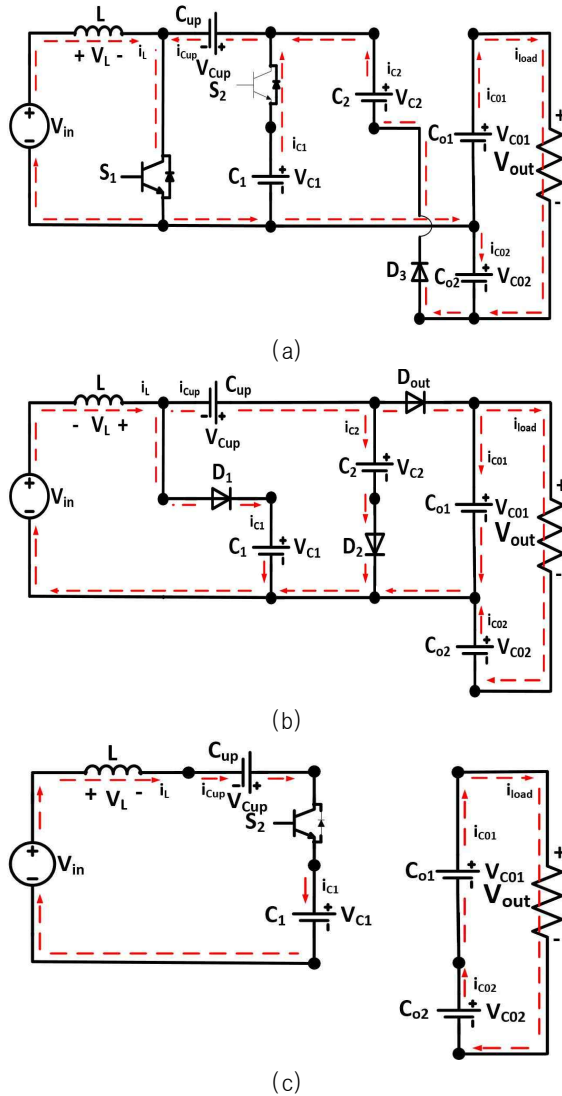


Fig. 4. Energy flowing schemes of switching states: (a) “S1S2” = [10], (b) “S1S2” = [00], (c) “S1S2” = [01].

- ③ It is possible to get high step-up gain capability, even output power of the load is extremely high.

## 2.2. Operating principle of the proposed converter

In this part operating principle of the proposed converter in continuous conduction mode (CCM) is discussed. Two switches ( $S_1$  and  $S_2$ ) are operated in the same duty value, but their gate driving signals has  $180^\circ$  phase difference. There are three different switching states “ $S_1S_2$ ” = [10, 00, 01], where “0” means switch have OFF state and “1” means ON state for two switches with the same duty value. Switching sequence is “10 - 00 - 01 - 00 - 10”. As seen from the Fig. 3,  $S_1$  and  $S_2$  are operating only when  $D < 0.5$ . It means that the duty cycle of the proposed converter is limited in  $[0 < D < 0.5]$  interval. Energy flowing paths of each switching states of the

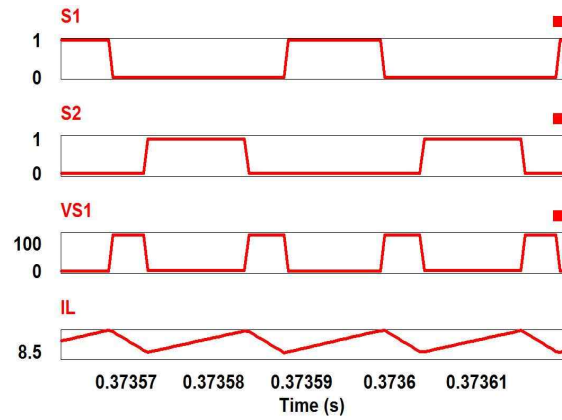


Fig. 5. Simulation results of the proposed converter. From top to bottom: gate signals for the  $S_1$  and  $S_2$  switches, drain-source voltage- $V_{S1}$  of the  $S_1$  switch and  $i_L$ - inductor current.

proposed topology are shown in Fig. 4 and also in Fig. 5, Fig. 6, Fig. 7 simulation results are shown.

In switching state “ $S_1S_2$ ” = [10]  $S_1$  is in ON state and oppositely  $S_2$  is in OFF state. In this switching state which can be seen in Fig. 4(a) inductor  $L$  is charged with linearly rising  $i_L$  current from input DC source and capacitor  $C_{UP}$  is charged by  $C_1$  and  $C_2$  capacitor. And also  $C_2$  and  $C_{o1}$  capacitors are discharged. The load is supplied by summarizing  $C_{o1}$ ,  $C_2$  and  $C_{up}$  capacitors voltages. Therefore, in this switching state the following equations are made:

$$V_L = V_{dcsource} = L^* \frac{dI_L}{dT} \quad (1)$$

$$V_{C_2} = V_{C_{UP}} + V_{C_{o2}} \quad (2)$$

$$V_{LOAD} = V_{C_{o1}} + V_{C_2} - V_{C_{UP}} \quad (3)$$

$$i_{LOAD} = i_{C_{o1}} + i_{C_2} - i_{C_{up}} \quad (4)$$

where

$V_{C_{UP}}$  is  $C_{UP}$  capacitor voltage;

$i_L$  is inductor current;

$V_{dcsource}$  is input DC source voltage;

$V_{C_1}$  is  $C_1$  capacitor voltage;

$V_{C_2}$  is  $C_2$  capacitor voltage;

$V_{C_{o1}}$  is  $C_{o1}$  capacitor voltage;

$V_{C_{o2}}$  is  $C_{o2}$  capacitor voltage;

$V_{LOAD}$  is the load voltage.

In the next “ $S_1S_2$ ” = 00 switching state both of the switches are in OFF state, which energy flowing

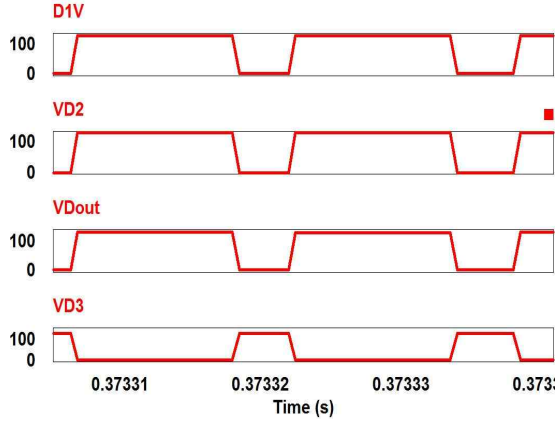


Fig. 6. Simulation results of the proposed converter. From top to bottom:  $D_1$ ,  $D_2$ ,  $D_{out}$  and  $D_3$  diodes stress voltages.

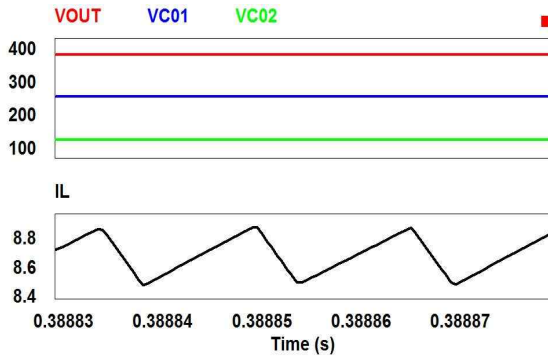


Fig. 7. Simulation results of the proposed converter. From top to bottom: output DC voltage-  $V_{OUT}$ (red),  $C_{o1}$  capacitor voltage-  $V_{C_{o1}}$ (blue),  $C_{o2}$  capacitor voltage-  $V_{C_{o2}}$ (green) and inductor current -  $i_L$ (black).

path is pictured in Fig. 4(b).  $C_{UP}$  and  $C_{o2}$  capacitors are discharged, the other  $C_1$ ,  $C_2$  and  $C_{o1}$  capacitors are charged. Diode  $D_3$  is turned off. The current of the inductor  $I_L$  is linearly decreased. In this switching state the load voltage is formed by summarizing input DC source, inductor,  $C_{UP}$  and  $C_{o2}$  capacitors voltages. The following equations are made in " $S_1 S_2$ " = 00 switching state :

$$V_{C_1} = V_{dcsource} - V_L \quad (5)$$

$$V_{C_2} = V_{dcsource} - V_L - V_{C_{UP}} \quad (6)$$

$$i_L = i_{C_1} + i_{C_2} + i_{C_{o1}} + i_{LOAD} \quad (7)$$

$$V_{LOAD} = V_{dcsource} - V_L - V_{C_{up}} - V_{C_{o2}} \quad (8)$$

In next  $S_1 S_2$ " = 01 switching state  $S_1$  is in OFF state and  $S_2$  is in ON state as shown in Fig. 4(c).  $D_{out}$  diode is turned off and the load is supplied in

accordance to the next equation :

$$i_{LOAD} = i_{C_{o1}} + i_{C_{o2}} \quad (9)$$

$$V_{LOAD} = V_{C_{o1}} + V_{C_{o2}} \quad (10)$$

In this switching state the load voltage is formed by summarizing  $C_{o1}$  and  $C_{o2}$  capacitors voltages, the inductor is charged by input DC source.  $i_L$  inductor current is linearly increased.

## 2.3 Operating analysis of the proposed converter

### 2.3.1 Voltage gain and duty cycle

From the above made equations (1-10) and applying volt-second balance of inductor during steady-state operation, the proposed converter main equations can be expressed as

$$V_{out} = \frac{3 * V_{dcsource}}{(1 - 2 * D)} \quad (11)$$

$$G = \frac{3}{(1 - 2 * D)} \quad (12)$$

$$i_L = \frac{3}{(1 - 2 * D)} * i_{load} \quad (13)$$

$$\Delta I_L = \frac{(1 - 2 * D) * V_{dcsource}}{L * f_{sw}} \quad (14)$$

where  $V_{out}$  is out DC voltage,  $G$  is voltage gain,  $i_L$  is average inductor current,  $\Delta I_L$  is inductor current ripple and  $V_{dcsource}$  is input DC source voltage of the proposed converter.

(12) equation shows that  $D$  duty value of the proposed converter should be within  $[0 < D < 0.5]$  interval. In traditional step-up converters, when high gain is required, the duty cycle should be in  $[0 < D < 1.0]$  interval. Using large duty cycles lead to high conduction and high switching losses. So, the proposed topology can earn high gain with a small duty cycle which can decrease conduction losses on the power semiconductors.

### 2.3.2 Voltage stress of the semiconductors

From (12), (13) and (14) equation, the maximum voltage stress of the semiconductors can be written as

$$V_{S1max} = V_{C_1} = \frac{1}{3} * V_{out} \quad (15)$$

$$V_{S2max} = V_{out} - V_{C_1} - V_{C_{o2}} = \frac{1}{3} * V_{out} \quad (16)$$

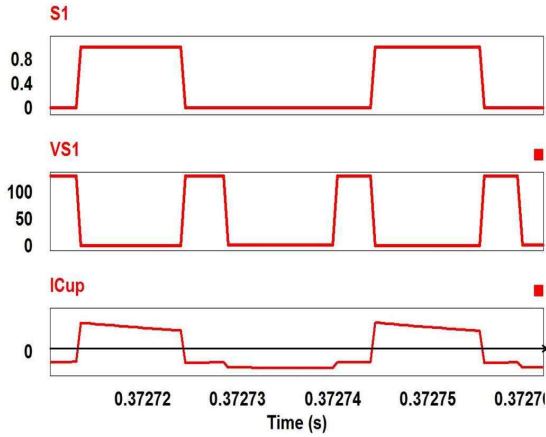


Fig. 8. Simulation results of the proposed converter. From top to bottom:  $S_1$  switch gate signal,  $S_1$  switch drain-source voltage-  $V_{S1}$ ,  $i_{C_{UP}}$ -capacitor  $C_{UP}$  current.

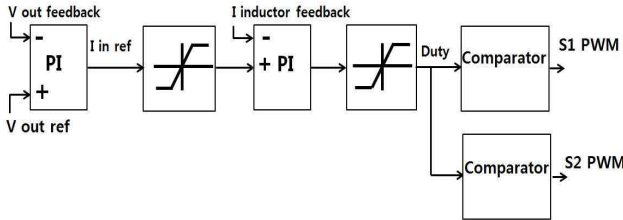


Fig. 9. Output DC voltage control scheme of the proposed topology.

$$V_{diode} = V_{S2max} = \frac{1}{3} V_{out} \quad (17)$$

where  $V_{S1max}$ ,  $V_{S2max}$ , are  $S_1$  and  $S_2$  switches maximum voltages and  $V_{diode}$  is diodes maximum voltages. Simulation waveforms of the diodes stress voltage are pictured in Fig. 6. It can be concluded that voltage stress all of the semiconductors is equal to third of the output voltage.

### 2.3.3 Output voltage control

As shown in Fig. 9, a double PI regulator is used to maintain output DC voltage in the reference voltage value range and to control input current. Duty value is being compared with the triangle waveform and thus PWM signals are made. Note that  $S_2$  switch PWM signal is made by phase shifting the triangle carrier waveform.

## 3. Simulation Results

To confirm the operating validity of the proposed topology, PWIM simulation was performed. The proposed boost dc-dc converter with 300W output is

designed and simulated by PSIM9.1 software tool. The simulation and experimental specifications of the proposed topology are described in Table II and Table III.

As shown from the Fig. 5,  $S_1$  switch  $V_{S1}$  drain-source voltage maximum value is equal to the third value of the output DC voltage. Inductor charged and discharged twice during one switching period. In the next Fig. 7 it is seen that  $V_{out}$  output DC voltage is formed by summing  $C_{o1}$  and  $C_{o2}$  capacitor voltages.

## 4. Comparison with Other High Gain Converters

### 4.1 Voltage gain

In nowadays there are many boost converters with high voltage gain, high efficiency, decreased duty cycle and decreased number of components. In order to compare the proposed topology with other step-up converters Table I is presented. As shown from the Table I, the proposed topology has higher voltage gain. And also the proposed topology requires the lowest duty cycle for the same voltage gain than converters in [5]–[11].

### 4.2 Active and passive components voltage stress and inductor current ripple

The voltage stresses of all power semiconductors in [5], [6], [10], [11] converters are between  $\frac{1}{2} V_{out}$  and  $\frac{2}{3} V_{out}$ . Converter in [7] has  $\frac{1}{3} V_{out}$  equal voltage stress, but it includes large number of components and operates in large duty cycle  $0 < D < 1.0$  as well as the other converters. In the proposed converter  $C_{o1}$  capacitor has  $\frac{2}{3} V_{out}$  equal voltage stress, but the other passive and active components have  $\frac{1}{3} V_{out}$  equal voltage stress. Moreover, inductor current frequency of the proposed converter is double the switching frequency which can reduce the input current ripple.

### 4.3 The number of active and passive components

Compares to converters in [7] and [10], the proposed topology uses less number of the components. Compares to converters in [7] and [10], the proposed topology uses less number of the components. Converter in [5] uses one less active

TABLE I  
COMPARISON BETWEEN THE PROPOSED CONVERTER AND OTHER CONVERTERS

Converters	Active elements (switch, diodes)	Passive elements (Cap, inductor)	Experimented power, W	Voltage gain	Voltage stress for switches
in [5]	5	7	40	$\frac{2}{1-D}$	$\frac{1}{2} * V_{out}$
in [6]	5	5	130	$\frac{D^2-3D+3}{(1-D)^2}$	$\frac{2}{3} * V_{out}$
in [7]	8	6	1000	$\frac{3}{1-D}$	$\frac{1}{3} * V_{out}$
in [10]	8	8	200	$\frac{4}{1-D}$	$V_{out} - V_{dsource}$
in [11]	5	3	100	$\frac{1+D_1}{1-D_1-D_2}$	$\frac{1}{2} * V_{out}$
proposed	6	6	300	$\frac{3}{1-2*D}$	$\frac{1}{3} * V_{out}$

TABLE II  
SIMULATION AND EXPERIMENTAL PARAMETERS OF THE PROPOSED CONVERTER

Parameter	Values
Input Voltage	36-72 V
Output Voltage	382 V
Power	300 W
Switching frequency	20 KHz
Efficiency	90 - 95 %

component, but it has one more passive component and experimented power is very low. Converter in [6] has one less active and one less passive component, but the duty cycle of the converter is very large. Converter in [11] has the decreased components, but as converter in [6] has high duty cycle. Therefore, the size and the weight of the proposed converter are lower than the other topologies.

## 5. Active and Passive Components Selection

### 5.1 Switches selection

Due to the proposed converter has decreased voltage stress for switches, all of the semiconductors are selected with maximum 200V breaking voltage capability.  $R_{DS(OV)}$  for Power MOSFET is selected lower than 10mOhm in order to decrease switching and conduction losses.

### 5.2 Passive components selection

The inductance of the proposed converter is selected by considering the input current ripple as 1 A and according to (18)

TABLE III  
ACTIVE AND PASSIVE ELEMENTS SPECIFICATION OF THE PROPOSED CONVERTER

Devices	Model	Specifications
MOSFET (S1, S2)	IRFP4668PBF	200V/130A
Diodes	DPG10I200PA/ IXYS	200V/10A
Capacitor	B43630F2827M000/TDK	820uF/250VDC
Capacitor	SAMYOUNG	470uF/250VDC
Inductor	TDK	720uH

$$L = \frac{(1-2*D)*V_{dsource}}{\Delta I_L * f_{sw}} \quad (18)$$

So, the minimum inductance value should be 600  $\mu H$ . The capacitance should be selected as

$$C_{min} = \frac{(1-2*D)*P_{out}}{\Delta V_{out} * V_{out} * f_{sw}} \quad (19)$$

Setting  $\Delta V_o$  out DC voltage ripple to 50mV and out DC voltage to 382 V, the minimum capacitance is calculated as  $C_{min} = 256\mu F$ . In this case to avoid a large out voltage ripple when the load power suddenly changes, the out capacitance is selected as  $C_{out} = 820\mu F$  per capacitor.

## 6. Experimental Results and Analyses

To verify output performance of the proposed converter, 300 W experiment prototype of the proposed converter was built as pictured in Fig. 10 and experiments were carried out. Two power switches IRFP4668PbF and four diode DPG10I200PA

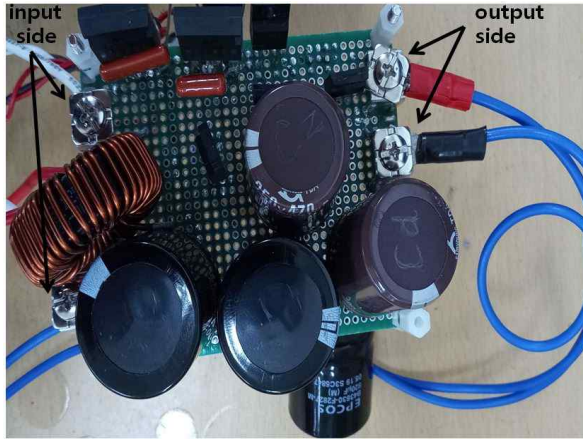


Fig. 10. Hardware prototype of the proposed converter.



Fig. 11. Control system of the proposed converter based on TMS320F28377S.

were used. The proposed converter is fed by KEYSIGHT N8762A power supply. Closed-loop control method as described in Fig. 9 is implemented by using DSP TMS320F28377S as pictured in Fig. 11. Resistor is used as the load. Experiment results are demonstrated in Fig. 12 - Fig. 16. Experiment and components parameters are shown in Table II and Table III. Applying the double closed-loop control method, the proposed topology normally operates under input DC voltage from 36 V to 72 V, out DC voltage  $V_{out} = 382V$  and out power  $P_{out} = 300W$ . Operating experiment waveform of the inductor  $L$  is the same as the simulation waveform: its charging and discharging frequency is double the switching frequency which is seen in Fig. 13. and Fig. 15.

When the proposed converter operates at the rated  $P_{out} = 300W$  power, its voltage stress of the power semiconductors are the third of  $V_{out}$  value which are seen from the Fig. 13, Fig. 14, Fig. 15.

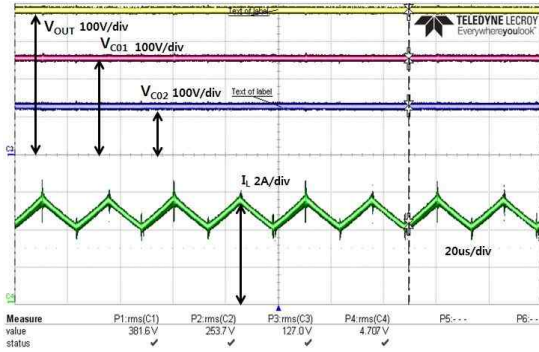


Fig. 12. Experiment results of the proposed topology. From top to bottom: output DC voltage -  $V_{OUT}$  (yellow),  $C_{o1}$  capacitor voltage -  $V_{C_{o1}}$  (red),  $C_{o2}$  capacitor voltage -  $V_{C_{o2}}$  (blue) and inductor current -  $i_L$  (green).

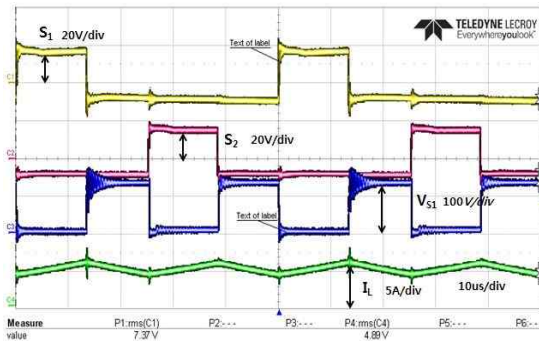


Fig. 13 Experiment results of the proposed topology. From top to bottom: gate signals for the  $S_1$  (yellow) and  $S_2$  (red) switches, drain-source voltage  $V_{S1}$  (blue) of the  $S_1$  switch and  $i_L$ -inductor current (green).

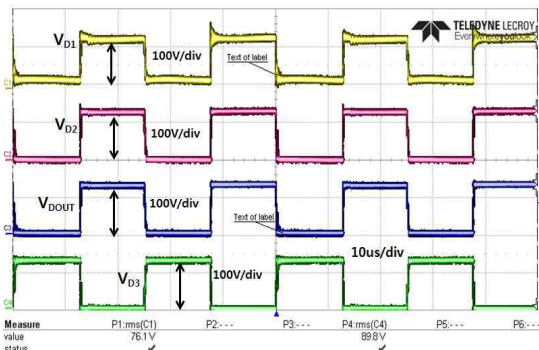


Fig. 14. Experiment results of the proposed topology. From top to bottom:  $V_{D1}$ ,  $V_{D2}$ ,  $V_{Dout}$ ,  $V_{D3-D1}$  (yellow),  $D_2$  (red),  $D_{out}$  (blue) and  $D_3$  (green) diodes stress voltages.

Fig. 12 shows  $V_{out}$ ,  $C_{o1}$ ,  $C_{o1}$  capacitors voltage waveforms where  $V_{out} = 382V$ ,  $C_{o1}$  capacitor holds  $\frac{2}{3} V_{out}$  equal and  $C_{o2}$  capacitor holds  $\frac{1}{3} V_{out}$  equal voltage value, which confirm that the proposed topology has multi level output capability. Some differences between the simulation results and the experimental

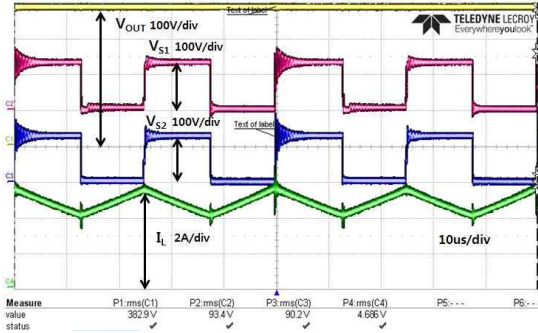


Fig. 15. Experiment results of the proposed topology. From top to bottom: output DC voltage  $-V_{OUT}$  (yellow), drain-source voltage  $-V_{S1}$  (red) of the  $S_1$  switch, drain-source voltage  $-V_{S2}$  (blue) of the  $S_2$  switch and  $i_L$  - inductor current (green).

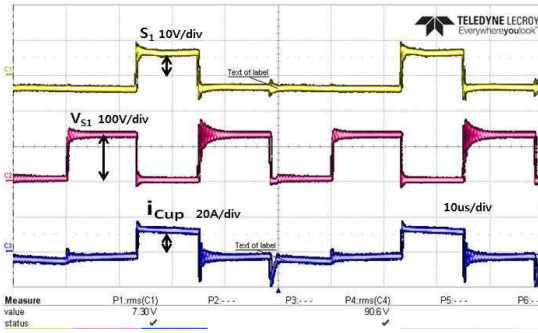


Fig. 16. Experiment results of the proposed topology. From top to bottom:  $S_1$  switch gate-source voltage (yellow),  $S_1$  switch drain-source voltage  $-V_{S1}$  (red) and  $C_{UP}$  capacitor current  $-i_{CUP}$  (blue).

waveforms are resulted due to the existence of  $ESR$  of the passive components and  $R_{DS(ON)}$  of the MOSFETs.

The output voltage stays invariable in reference voltage value of 382 V when input voltage changes from 36 V to 72 V. It means that the proposed topology can achieve voltage gain from 5.3 to 10.6. Relatively to changes in input voltage, the duty cycle of the proposed converter changes from 0.23 to 0.372 which avoid extreme duty cycle changes. Waveform of diodes voltages is presented in Fig. 14. As it is seen the maximum value of the voltage does not extend the  $\frac{1}{3} V_{out} = 127.3V$  value. The  $C_{UP}$  capacitor current waveform is shown in the Fig. 16. As shown from the waveform the  $C_{UP}$  capacitor charges when  $S_1$  switch is in ON state and discharges when  $S_1$  switch is in OFF state. The most important fact that the  $C_{UP}$  capacitor has no inrush current.

Experiments also were conducted to measure efficiency of the proposed converter at different input

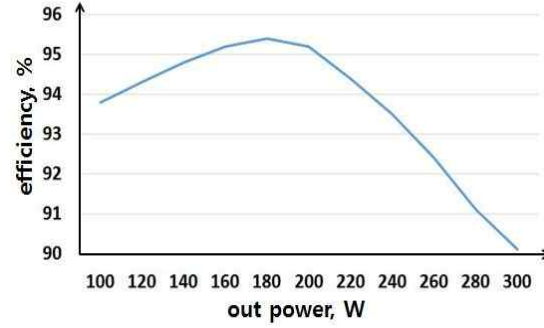


Fig. 17. Efficiency-out power curve when  $V_{dsource} = 36V$ .

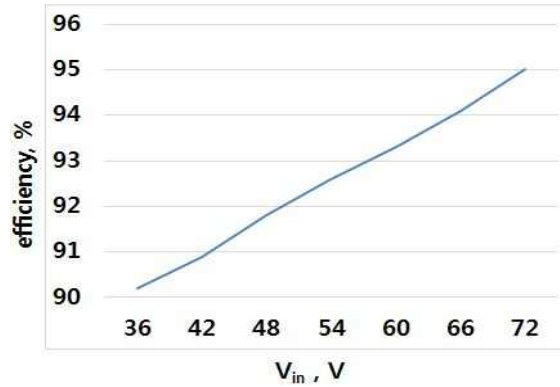


Fig. 18. Efficiency - input voltage curve when  $P_{OUT} = 300W$ .

voltages and at different output power. Efficiency - out power curve waveform is presented in Fig. 17. Differences between the simulation and the experimental efficiency is around 1%. The maximum efficiency is 95.1% when input voltage is 72V and the rated power is 300W. The minimum efficiency is 90% at 36V input and at 300W out power. Efficiency decreasing reason is due to the increasing power losses caused by the input current. From the Fig. 18 it is seen that by decreasing input voltage the efficiency value is also decreased.

## 7. Conclusions

In this paper a new multi level high gain boost DC-DC converter with wide input voltage range and reduced stress voltage capability is proposed. The main advantages of the proposed topology are as follows:  $\frac{1}{3} V_{out}$  equal voltage stress, multi level voltage output capability and low conduction losses on the semiconductors. And also small duty cycle in  $[0 < D < 0.5]$  interval can be used for achieving high voltage gain when the input voltage varies between 36V to 72V. Furthermore, the inductor of the proposed



converter is charged and discharged twice during one switching period. As a result, input current ripple is decreased. A lot of experimental results proved that the proposed converter could be used as high gain DC-DC power conversion system to coordinate low voltage PV or fuel cell stacks with high 380V DC buses.

## References

- [1] Sh. R. Pasha and B. Mallika, "A new hybrid boosting converter for renewable energy applications," *International Journal of Advanced Technology and Innovative research*, Vol. 8, No. 19, pp. 2348-2370, Nov. 2016.
- [2] Y. Hu, J. Wu, W. Cao, W. Xiao, P. Li, S. J. Finney, and Y. Li, "Ultrahigh step-up DC-DC converters for distributed generation by three degrees of freedom (3DoF) approach," *IEEE Transactions on Power Electronics*, Vol. 31, No. 7, pp. 4930-4941, Jul. 2016.
- [3] A. Priyadarshi, P. K. Kar, and S. B. Karanki, "Switched capacitor based high gain DC-DC converter topology for multiple voltage conversion ratios with reduced output impedance," *Journal of Power Electronics*, Vol. 19, No. 3, pp. 676-690, May. 2019.
- [4] M. Forouzesh, Y. P. Siwakoti, S. A. Gorji, F. Blaaberg, and B. Lehman, "Step-up DC-DC converters: A comprehensive review of voltage-boosting techniques, topologies and applications," *IEEE Transactions on Power Electronics*, Vol. 32, No. 12, pp. 9143-9178, Dec. 2017.
- [5] E. H. Ismail, M. A. Al-Saffar, A. J. Sabzali, and A. A. Fardoun, "A family of single-switch PWM converters with high step-up conversion ratio," *IEEE Trans. Circuits Syst. I, reg. Papers*, Vol. 55, No. 5, pp. 1159-1171, May. 2008.
- [6] S. S. Lee, B. Chu, C. S. Lim, and K. Y. Lee, "Two-inductor non-isolated DC-DC converter with high step-up voltage gain," *Journal of Power Electronics*, Vol. 19, No. 5, pp. 1069-1073, Sep. 2019.
- [7] Y. J. A. Alcazar, D. S. Oliveira Jr, F. L. Tofoli, and R. P. Torrico-Bascope, "DC-DC nonisolated boost converter based on the three-state switching cell and voltage multiplier cells," *IEEE Trans. Ind. Electron*, Vol. 60, No. 10, pp. 4438-4449, Oct. 2013.
- [8] B. Honarjoo, S. M. Madani, M. Nirooman, and E. Adib, "Analysis and implementation of a new single switch , high voltage gain DC-DC converter with a wide CCM operation range and reduced components voltage stress," *Journal of Power Electronics*, Vol. 18, No. 1, pp. 11-22, Jan. 2018.
- [9] K. C. Tseng, C. C. Huang, and C. A. Cheng, "A high step-up converter with voltage-multiplier modules for sustainable energy applications," *IEEE Transactions on Power Electronics*, Vol. 3, No. 4, pp. 1100-1108, Dec. 2015.
- [10] S. Z. Chen, Z. Wang, S. S. Yu, G. Zhang, and Y. Zhang, "A novel alternative to traditional nHSLC: An n-switched-cell based approach to high-step-up converters," *IEEE Access*, Digital Object Identifier 10.1109/ACCESS.2019.2935753.
- [11] M. Lakshmi and S. Hemamalini, "Nonisolated high gain DC-DC converter for DC microgrids," *IEEE Transactions On Industrial Electronics*, Vol. 65, No. 2, pp. 1205-1212, Feb. 2018.
- [12] G. Zhang, B. Zhang, Z. Li, D. Qiu, L. Yang, and W. A. Halang, "A 3-Z-network boost converter," *IEEE Trans. Ind. Electron*, Vol. 62, No. 1, pp. 278-288, Jan. 2015.



### Ibadullaev Anvar

He was born in 1978 in Uzbekistan. He received the B.S. degree in electronics and automation from Tashkent State Technical University in 2012 and the M.S. degree in Electrical engineering from Chonnam National University, Gwangju, South Korea, in 2015. He is currently pursuing the Ph.D. degree in Electrical engineering at Chonnam National University, Gwangju, South Korea. Since 2016, he has been working as Senior Research Assistant in the field of Power Electronics at Power Conversion Lab. at EDS Co, South Korea.



### Sung-Jun Park

He was born in 1965 in South Korea. He received the B.S., M.S., and Ph.D. degrees in electrical engineering and the Ph.D. degree in mechanical engineering from Pusan National University, Busan, South Korea, in 1991, 1993, 1996 and 2002, respectively. From 1996 to 2000, he was an Assistant Professor with the Department of Electrical Engineering, Koje College Geoje, South Korea. From 2000 to 2003, he was an Assistant Professor with the Department of Electrical Engineering, Tongmyong College, Busan. Since 2003, he has been working as Professor with the Department of Electrical Engineering, Chonnam National University, Gwangju, South Korea.